

Wright State University

CORE Scholar

---

Biomedical, Industrial & Human Factors  
Engineering Faculty Publications

Biomedical, Industrial & Human Factors  
Engineering

---

6-27-2022

## Effectiveness of Mesoporous Bioglass in Drug Delivery

Sheila Galbreath

Bailey Krueger

Taylor Frazier

Tarun Goswami

Wright State University - Main Campus, tarun.goswami@wright.edu

Follow this and additional works at: <https://corescholar.libraries.wright.edu/bie>



Part of the [Biomedical Engineering and Bioengineering Commons](#), and the [Industrial Engineering Commons](#)

---

### Repository Citation

Galbreath, S., Krueger, B., Frazier, T., & Goswami, T. (2022). Effectiveness of Mesoporous Bioglass in Drug Delivery. *Journal of Pharmaceutical and Biopharmaceutical Research*, 4 (1), 271-282.  
<https://corescholar.libraries.wright.edu/bie/205>

This Article is brought to you for free and open access by the Biomedical, Industrial & Human Factors Engineering at CORE Scholar. It has been accepted for inclusion in Biomedical, Industrial & Human Factors Engineering Faculty Publications by an authorized administrator of CORE Scholar. For more information, please contact [library-corescholar@wright.edu](mailto:library-corescholar@wright.edu).

## RESEARCH ARTICLE

## Effectiveness of mesoporous bioglass in drug delivery

Sheila Galbreath<sup>1</sup> Bailey Krueger<sup>1</sup> Taylor Frazier<sup>1</sup> Tarun Goswami<sup>1\*</sup><sup>1</sup> Department of Biomedical, Industrial and Human Factors Engineering, Wright State University, Dayton, OH 45435, USA

**Correspondence to:** Tarun Goswami, Department of Biomedical, Industrial and Human Factors Engineering, Wright State University, Dayton, OH 45435, USA; Email: [tarun.goswami@wright.edu](mailto:tarun.goswami@wright.edu)

**Received:** May 16, 2022;

**Accepted:** June 24, 2022;

**Published:** June 27, 2022.

**Citation:** Galbreath S, Krueger B, Frazier T, *et al.* Effectiveness of mesoporous bioglass in drug delivery. *J Pharm Biopharm Res*, 2022, 4(1): 271-282. <https://doi.org/10.25082/JPBR.2022.01.004>

**Copyright:** © 2022 Sheila Galbreath *et al.* This is an open access article distributed under the terms of the [Creative Commons Attribution License](https://creativecommons.org/licenses/by-nc/4.0/), which permits unrestricted use, distribution, and reproduction in any medium, provided the original author and source are credited.



**Abstract:** Since the invention of bioactive glass 50 years ago, it has become a versatile material used in healthcare in a variety of applications and compositions. Bioactive glass has shown superior capabilities of drug delivery compared to traditional carriers. For example, time-released medications are less likely to reach toxic levels, while delivering a specific, therapeutic dose to a localized area. The objective of this paper is to investigate the properties and effectiveness of mesoporous bioglass (MBG) as a drug delivery carrier. A literature review of various polymer coated 45S5 Bioglass<sup>®</sup> loaded with vancomycin was analyzed to determine their drug release response. Since MBG continues to be a preferred carrier with numerous combinations; size, coating, doped with ions, medications, and other physical conditions, there is a need to understand more fully their effectiveness. For a given loading efficiency of 5-15% the burst release % for day 1 remained 15-30% for given surface area, pore volume and pore size of 3.5 to 5 nm. The mechanical properties summarized in this paper are compared with the drug release kinetics. In general, for a given fracture toughness and compressive strength, the ratio of Young's modulus to bending strength around 250 determined poor apatite mineralization resulting in slow release. As this ratio increased the apatite mineralization and dissolution rate increased. Doping MBG with ions enhanced the drug efficacy to treat a particular condition, for example, silver. Polymer coated MBG exhibited slower dissolution rate than uncoated MBG. Dissolution time increased with the drug loading rate, drying time of the coating, multi-layer coats of drug and polymer for the drug studied in this paper to more than 50%.

**Keywords:** dissolution, kinetics, MBG, polymer coats, loading rate, time to release

## 1 Introduction

In 1969, Larry Hench created 45S5 Bioglass<sup>®</sup> with the purpose of developing a material that would not be rejected in a biological environment or encapsulated to protect the native tissue [1]. During this time, many soldiers were returning home from the war with a variety of orthopedic injuries, such as amputations, bone and tissue damage. Before the discovery of Bioglass<sup>®</sup>, standard practice in orthopedics was to select implants made with various steel alloys based on their corrosion resistance. In many instances, implants were rejected due to material sensitivity [2]. As a result, premature failure occurred within two months due to encapsulation of the implant with macrophage and metallic ions [3]. 45S5 Bioglass<sup>®</sup> is the first synthetic material to form a chemical bond with bone; that body did not reject [2]. The creation of Bioglass<sup>®</sup> gave physicians an alternative implant that was both biodegradable and biocompatible with the host tissue [2].

Bioactive glass has become one of the most versatile materials used in healthcare, which has spurred research and development, with numerous applications and formularies [2]. The unique properties of this ceramic have made it a popular product with several uses such as treating bone injuries, wound therapy, tissue engineering applications, bone infections, cranial and bone repair, toothpaste, and drug delivery [1]. Since 1969, many variations of the original formula of 45SiO<sub>2</sub>-24.5Na<sub>2</sub>O-24.5CaO-6P<sub>2</sub>O<sub>5</sub> (wt%), have been formulated based on their application [1, 3]. Developments in Bioactive glass were summarized in literature put together in timeline diagram in Figure 1.

Bioglass<sup>®</sup> is a desirable and versatile product because of its ability to be incorporated and accepted by natural bone by developing a covering of hydroxyapatite formation (necessary in mineralization of native bone), while encouraging the injured site to heal [1]. The bond between synthetic material, Bioglass<sup>®</sup> and the natural bone is so strong that a separation can only happen by fracture [2]. The bond strength between the bioglass and bone is naturally occurring apatite (hydroxyapatite (Ca<sub>5</sub>(PO<sub>4</sub>)<sub>3</sub>OH), an osteoconductive material [8,9]. During the bone's healing process, the bioglass degrades, allowing for the controlled release of ions and medications at the

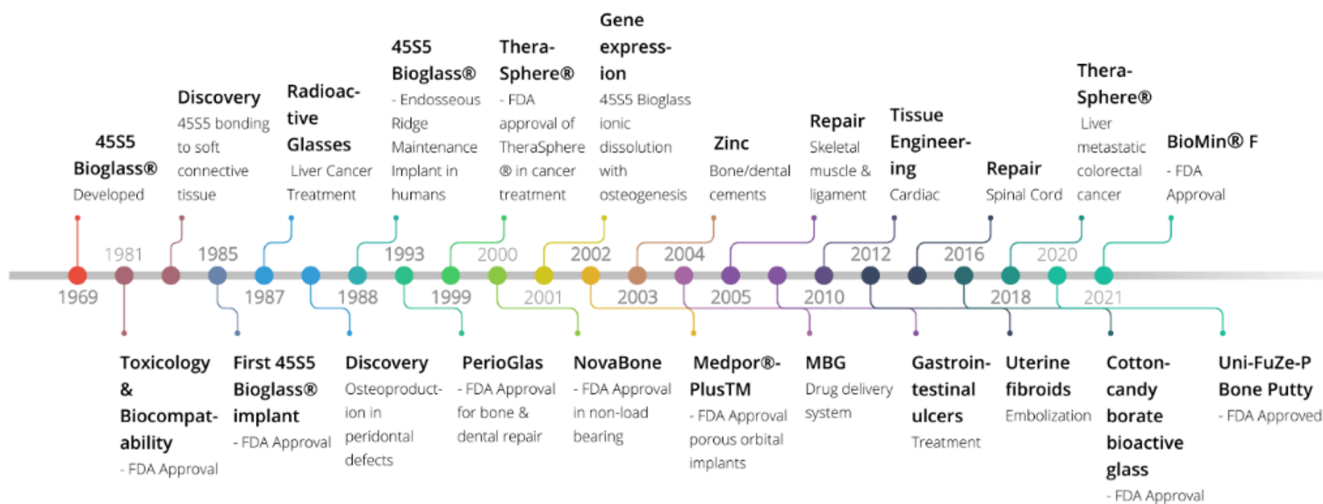


**Figure 1** Time-line of noteworthy applications of bioglass from 1969 to 2021 [1,4–7]

injured site [8]. Review of role of ions, morphology, polymers and mechanical properties of the bioglass conducted together with applications of mesoporous bioactive glass (MBG) in drug delivery.

### 1.1 Mesoporous Bioactive Glass (MBG) overview

Although there are numerous additive manufacturing options to fabricate the biomaterial, 3D- printing macro-mesoporous scaffolds with the incorporation of poly (vinyl alcohol) have shown to have great promise, resulting in mineralization, ability to release drugs, while having a 16 MPa compressive strength [1]. 3D printing provides the ability of incorporation options into the MBG, various polymer, biomaterial options, inorganic and organic material [1]. 3D MBG (80SiO<sub>2</sub>–15CaO–5P<sub>2</sub>O<sub>5</sub> (mol%)) was loaded with gentamicin and demonstrated twice as much drug loading with a reduction in release rate compared to traditional BG; thereby showing superior attributes [1]. In order to prevent tissue toxicity, the challenge of controlling the release rate of MBG must be addressed by the addition of incorporating a biodegradable polymer to the medication [1].

MBG is a drug delivery carrier, has increased surface area and pore-volume, with pore uniformity via mesoporous channels that assist in drug loading [1, 10]. An MBGs volume in the pores and surface is directly related to the MBGs amount seen in the loading efficiency of therapeutic drugs (i.e. growth factors, drugs etc.) [11]. Figure 2 compares the structure and function on a macro- and micro- scale of scaffolds of bioactive glass (A, B, C) and native calcined cancellous bone (D, E, F) [12].

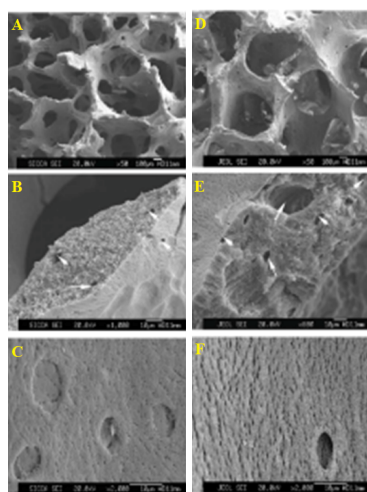


**Figure 2** SEM images of macro- and micro- structure and function of bioactive glass scaffold (A, B, C) and native calcined cancellous bone (D, E, F) [12].

Figure 2 A to F are images of the macro- and micro- scaffold of bioactive glass and native calcined cancellous [12]. A comparison between Figure 1A (bioactive glass) to Figure 1B (calcined cancellous bone) depicts similar interconnectedness and the number of pores [12]. The porosity % of bioactive glass is 89.3 ± 2.0 and 86.6 ± 1.5 [12, 13].

## 2 MBG in drug delivery

The use of MBGs as a drug delivery mechanism allows the medication to be directly administered to the affected area while decreasing the risk of toxicity that may result in adverse systemic effects [14]. Drawbacks of traditional delivery of medication is device failure, adverse effects from long term medication exposure, increased healthcare costs and medical procedures [15]. MBGs are preferred to other bioglass options, because of its superior mechanical properties such as its structure and increased surface area; as well as reducing the negative effects of traditional medication administration that are released quickly [15]. The MBG with a medication is controlled release of the drug by the route of a porous scaffold, using the mechanism of diffusion to support and expedite both osteogenesis and angiogenesis necessary for orthopedic healing [15, 16]. A condensed summary of variations of MBGs used as a drug carrier is listed in Table 1. The process of placing the biomaterial on the bone begins with the drug/growth factor/ions added to the MBG, which leads to the MBG covering the drug/growth factors/ions then adding that to the polymer, to make a polymer covered in the MBG/loaded agent [16]. The biomaterial is applied to the location of the bone injury, thereby facilitating healing with the release of the therapeutic loading agent [16].

### 2.1 MBG drug carrier summary

An attempt was made to summarize various MBG compositions with or without the use of growth factors and types, with the drug loading rate or efficiency, burst release in 1 day, delivery time in days, surface area of the carrier, pore volume used for each MBG combination, together with the pore size in Table 1.

**Table 1** Drug/Growth and Composition of MBG [11, 14]

MBG Composition	Drug/growth factor	Loading efficiency (%)	Burst rel. (% day 1)	Deliver Time (days)	Surface area (m <sup>2</sup> g <sup>-1</sup> )	Pore vol. (cm <sup>3</sup> g <sup>-1</sup> )	Pore Size (nm)
80Si15Ca5P	ibuprofen	35	25-45,90	>10	317-351	0.36-0.37	3.7-4.8
80Si15Ca5P					351	0.49	4.6
80Si15Ca5P	ipriflavone	1-11		>10	317-351	0.36-0.37	3.7-4.8
100Si	Tetracycline	10-18	15-30	>5	310-490	0.356-0.4	4.2
100Si					310-490		3.6-4.2
90Si5Ca5P	metoclopramide	15-45	40-55	>5	330	0.35	4.9
90Si5Ca5P					330	0.35	4.9
95Si5Ca					467		3.7
80Si15Ca5P	phenanthrenr			>5	317-351	0.36-0.37	3.7-4.8
80Si15Ca5P					351	0.36	4.8
70Si15Ca5P					319	0.49	4.6
60Si15Ca5P					310	0.43	4.3
70Si25Ca5P				>5	303-319	0.33-0.49	4.6-4.8
100Si	triclosan	9.1-10.7	30	>14	351	351	351
85Si10Ca5P	Ibuprofen, bovine serum albumin	20	100	>14			
90Si10Ca	-				438		3.5
70Si25Ca5P	gentamicin	5.5-14.4	60-80	>4	303-319	0.33-0.49	4.6-4.8
80Si15Ca5P	gentamicin	11	70	>7	317-351	0.36-0.37	3.7-4.8
80Si15Ca5P					265-515	0.36-0.49	3.62-5.29
80Si15Ca5P	dexamethasone	16	20-50	>7	317-351	0.36-0.37	3.7-4.8
80Si15Ca5P	VEGF	90	0.2	>7	317-351	0.36-0.37	3.7-4.8
100Si	BMP			>7	310-490	0.356-0.4	4.2
80Si15Ca5P	Gentamicin/Nap-roxen	1.1	30-50	>10	317-351	0.36-0.37	3.7-4.8
80Si15Ca5P	dexamethasone	54	50	>10	317-351	0.36-0.37	3.7-4.8
80Si10Ca5P5Fe					260	0.26	3.5
80Si5Ca5P10Fe					334	0.3	3.6
80Si0Ca5P15Fe					367	0.36	3.7
80Si10Ca5P5Mg					274	0.35	3.31
80Si10Ca5P5Zn					175	0.23	3.33
80Si10Ca5P5Cu					237	0.31	3.66
80Si10Ca5P5Sr					247	0.31	3.66
76.5Si15Ca5P3.5Ce					397	0.38	2.9
76.5Si15Ca5P3.5Ga					335	0.31	3.8
75Si15Ca5P5B					234	0.24	5.28
70Si15Ca5P10B					194	0.21	5.09
80Si10Ca5P5Zr					287	0.32	3.7
80Si5Ca5P10Zr					278	0.33	4.1
80Si5P15Zr					277	0.27	3.4

The loading efficiency value reflects the encapsulation efficiency of the medication, that the bioglass is carrying [17, 38]. Burst release is the moment the medication-infused bioglass releases the medication through dissolution [18]. After the initial release of medication, the rate of delivery will be predictable [18]. At this junction, there is little understanding of the mechanism of burst releases [18]. MBG's elevated amount of Si-OH provides positive effects on reducing and prolonging the drug kinetics [11].

The relationship between surface area, particle size, porosity, and texture of the material should be noted [19]. As the particle size decreases, the surface area increases, thus allowing more medication to be exposed and released [19]. The surface area can exceed what the particle size is when it has small pores [19]. A rough powder can have a smaller surface area compared to a finer powder, because materials with small pores have a larger surface area [19]. The surface area is one of many factors in determining the rate of the dissolution of bioglass [19]. The International Union of Applied Chemistry (IUPAC) listed MBG to have a porosity within the range of 2-50 nm [11].

Pore volume is the amount of volume a substance will fill within a specified space [20]. IUPAC listed MBG to have an approximate pore volume of 1 cm<sup>3</sup>/g [11]. If the pore size is less than 100 micrometers, blood and oxygen cannot reach the site of injury so that cartilage will grow instead of bone [3]. The ideal pore size to encourage bone growth and blood flow should be greater than 200 - 300 micrometers [3]. MBGs stick to the area it is placed on a cellular level due to its large surface area, pore volume and organized mesoporous pattern [15]. The downside to the larger pore size is the Young's Modulus will resemble closer to trabecular bone [3]. The amount of blood, oxygen, and strength should be taken into consideration when determining the optimal pore size, based on its intended application [3]. A balance must be found between finding the optimal pore size while maximizing its mechanical properties [21]. A high-resolution TEM image of the mesoporous silica is shown in Figure 6. The uniformity of the MBG can be controlled by the fabrication of the material depending on the surfactant used, resulting in uniformity of the pore size between 2-30 nm [11].

## 2.2 Role of ionizing MBGs

The numerous benefits of ions range from helping in vascularization to encouraging new bone formation [8]. As the bioglass dissolves and the ions are released; the injury is directly treated with therapeutic properties of the ions, while minimizing side effects [8]. When the rate of dissolution is controlled, therapeutic levels of ions and medications can be achieved [22]. Controlling the dissolution rate is important to prevent toxicity from some ions, like zinc [8]. Table 2 summarizes a list of ions and their benefits when incorporated into bioglass.

## 2.3 Summary of ions role

**Table 2** Summary of benefits realized with ions incorporated with bioglass [1, 8, 11, 23, 24]

Ions	Benefits	Concentration (mg/L) in MBG
Calcium – Osteogenesis/ angiogenesis	Osteoblast differentiation Apatite precipitation Promotes endothelial cell proliferation SMAD—bone remodel role (osteoblasts and osteoclasts)	
Strontium	Osteoblast – encourage cells for bone forming Osteoclasts - prevent reabsorbing bone Decrease osteoclastic → increase Sr <sup>2+</sup>	<22
Silver (Ag) – Antibacterial	Antibacterial ability - interrupt the function of bacterial cell membrane – (ie. Escherichia coli, Pseudomonas aeruginosa, and Staphylococcus aureus) Bacteriostatic and bactericidal to many pathogens' bacteria Does not develop bacterial resistance Non toxic to osteoblasts Bacterial cell membrane protons released	0.014
Fluoride – osteogenesis	Fluorapatite - prevent dental cavities, encourage bone growth & prevent osteoporosis fracture Fluorapatite surface layer – preforms similar to a protective layer by decreasing ion release Osteogenesis	
Zinc	Wound healing - bactericidal Cytotoxic – with high concentrations Release is pH-dependent	<0.75
Magnesium	Vascularization Encourage new bone formation Angiogenesis – form blood vessels via hypoxia	<100
Cobalt	Material that preforms similar to treatments to mimic hypoxia used in regenerative medicine	<25
Copper, Nickel	Material that preforms similar to treatments to mimic hypoxia used in regenerative medicine	
Silicon	Osteoblast – encourage differentiation and proliferation	
Borate	May encourage RNA synthesis in fibroblasts	<50
Copper	Antimicrobial agents - against some gram-negative, gram-positive bacteria Toxicity low Bone formation and healing important Wound healing and bone regeneration	<152
Lithium – Osteogenesis	Osteogenesis	<17.28

## 2.4 Polymers

The addition of polymer to bioglass composite has many positive benefits to the material and a drug delivery system. The medication will adhere to the polymer, thereby delivering long term medication to a localized area and administrating long term medication [14]. Polymers used in bioglass would bypass the risks associated with long term use of traditional medicinal therapies [25].

### 3 Mechanical properties

The polymer positively contributes to the composite's mechanical properties, by making the material tougher and the interface stronger [25, 26]. Coating bioglass in a polymer is more desirable to use in load bearing applications, because it offsets the brittleness observed in uncoated bioglass. A polymer coat will seal the scaffolds of the bioglass of any existing defects of the material, resulting in decreasing the likelihood of a crack formation. A common, biodegradable polymer used is Polycaprolactone (PCL) because it is easy to manufacture and its mechanical properties meet minimum requirements [26].

By incorporating polymers, the mechanical properties of the bioglass become closer to the bone's properties [9]. By comparing the compressive strength of 45S5 Bioglass<sup>®</sup> foam that was coated in polymer poly (3-hydroxybutyrate-co-3-hydroxyvalerate) (PHBV) with the 45S5 Bioglass without a coating, the polymer coating increased the compressive strength by 1.5 MPa [1, 3]. Polycaprolactone (PCL), chitosan, and PHBV are some of the most common polymers used in bioglass [4, 27]. Like ions, each type of polymer has its own set of desirable attributes that can be tailored based on its intended use. Regardless of which polymer is used, they should all be biodegradable, non-toxic, slowly reabsorbed into the body, have beneficial mechanical properties, and not contain hydrocarbons [5, 27].

#### 3.1 Mechanical properties of MBG and human bone

The closer the mechanical properties of the implant are to the host bone, the more likely it will be accepted by the natural bone through bonding, and less likely to be rejected [2, 9]. Table 2 compares the compressive modulus (GPa), compressive strength (MPa), fracture toughness ( $\text{MPa}\sqrt{\text{m}}$ ), bending strength, and Vickers hardness of bioactive glasses, ceramics and bone [9]. In general, the fracture toughness of bioactive glass as a whole is less than that of bone [9]. Table 2 shows that Cerabone<sup>®</sup> AW ( $34\text{SiO}_2-16.2\text{P}_2\text{O}_5-44.7\text{CaO}-0.5\text{CaF}_2-4.6\text{MgO}$  wt%) has the highest mechanical properties on the chart, making it an ideal material when compressive strength is required [9]. It is noteworthy to state that all synthetic material toughness is lower than natural bone [9]. When compared to the rest of the ceramics, hydroxyapatite (HA) has a fracture toughness of 0.8-1.2  $\text{MPa}\sqrt{\text{m}}$  and the bending strength of 60-120 MPa, but it is not as high as natural bone [9]. A summary of the mechanical properties of bioactive glass, ceramics and human bone can be found in Table 3 and 4 [9].

**Table 3** Mechanical properties of human bones [9, 28]

Material	Compressive modulus (GPa)	Compressive strength (MPa)	Fracture toughness ( $\text{MPa}\sqrt{\text{m}}$ )	Bending strength (MPa)	Vickers hardness (MPa)	Tensile Strength (MPa)
HA	35-120	100-150	0.8-1.2	60-120	90-140	
Trabecular bone	0.05-0.6	1.5-7.5	0.1-0.8	10-20	40-60	
Cortical bone	7-30	100-135	2-12	50-150	60-75	
Cancellous bone	0.5-0.05	2-12				10-20

##### 3.1.1 Properties for calcium silicate bioceramics

Table 3 lists bioglass variations and mechanical properties; whereas Table 4 provides information on both the mechanical properties of calcium silicate bioceramics, apatite mineralization and dissolution behavior. Table 3 shows that hydroxyapatite HA has a fracture toughness of 1.2  $\text{MPa}\sqrt{\text{m}}$  and the bending strength of 120 MPa, whereas the correlating values found in Table 4 for silicate bioceramics are higher [9]. The silicate bioceramics bending strength and elastic modulus are close to cortical bone [9]. Ceramic with high concentrations of calcium have better apatite mineralization [9]. The apatite mineralization decreased when magnesium, zinc, or zirconium was added to the calcium silicate ceramics [9]. The faster the bioglass dissolves, the better the apatite mineralization, indicating a linear relationship [9].

#### 3.2 Apatite mineralization

An apatite structure can be found in bones that have biominerals found in its chemical makeup [29]. All biomaterials have advantages and disadvantages in their design as it applies to their intended use. The benefits of Bioglass<sup>®</sup> were discussed in the introduction, but the drawbacks of this material is that it has lower mechanical strength and fracture toughness than the mechanical properties of bone [9]. To offset the fragility of bioglass, it has been mixed with polymers to increase its mechanical properties [21]. Bioglass has also been combined with a variety of biocompatible composites, to increase the properties [9]. It is important to understand



the specific mechanical properties of the bioglass so that all relevant information is available to determine how the material would be best applied to prevent harm [9].

An example can be seen in Table 2, in which Cerabone® AW has a compressive strength 1080 MPa, fracture toughness of 2 MPa  $\sqrt{m}$ , bending strength of 215 MPa, and Vickers hardness of 680 MPa [9]. The superior mechanical properties of this material make it a good option where higher compressive properties are required, such as a vertebral implant [9]. Biomaterials are not as tough as cortical bone [9].

**Table 4** Mechanical Properties of Calcium Silicate Bioceramics, and porous scaffolds.

Ceramic	Composition	Bending strength (MPa)	Elastic modulus (GPa)	Compressive strength (MPa)	Fracture Toughness (MPa $\sqrt{m}$ )	Apatite Mineralization	Dissolution behavior
Wollastonite	CaSiO <sub>3</sub>	294 <sup>a</sup> 9 <sup>5</sup>	46.5 <sup>a</sup>	60 60 <sup>b</sup> 0.4 <sup>c</sup> 3.6 <sup>d</sup>	2.0 <sup>a</sup>	Excellent	Rapid
Dicalcium silicate	Ca <sub>2</sub> SiO <sub>4</sub>	26-97 293 <sup>a</sup>	10-40		1.1-1.8 3.0 <sup>a</sup>	Excellent	Rapid
Tricalcium silicate	Ca <sub>3</sub> SiO <sub>5</sub>	93.4 293 <sup>a</sup>	36.7		1.93 3.0 <sup>a</sup>	Excellent	Rapid
Magnesium silicate	MgSiO <sub>3</sub>	32	8.5			Poor	Very slow
Dimagnesium silicate	Mg <sub>2</sub> SiO <sub>4</sub>	203			2.4	Poor	Very slow
Monticellite	CaMgSiO <sub>4</sub>	159	51		1.63	Moderate	Slow
Merwinite	Ca <sub>3</sub> MgSi <sub>2</sub> O <sub>8</sub>	151	31		1.72	Good	Moderate
Diopside	CaMgSi <sub>2</sub> O <sub>6</sub>	300		0.2-1.36	3.50	Moderate	Slow
Akermanite	Ca <sub>2</sub> MgSi <sub>2</sub> O <sub>7</sub>	—		0.53-1.13	0.63-1.72	Good	Moderate
Bredigite	Ca <sub>7</sub> MgSi <sub>4</sub> O <sub>16</sub>	156	43	0.233	1.57	Excellent	Rapid
Hardystonite	(Sr,Ca)SiO <sub>3</sub>	136	37		1.37	Poor	Very slow
Strontium hardystonite	Zn <sub>(x)</sub> CaSiO(3 + x)					Poor	Very slow
Baghdadite	Ca <sub>2</sub> ZnSi <sub>2</sub> O <sub>7</sub>						
Sphene	Sr <sub>2</sub> ZnSi <sub>2</sub> O <sub>7</sub>					Poor	Very slow
Silicocarnotite	CaNa <sub>2</sub> SiO <sub>4</sub> Ca <sub>2</sub> Na <sub>2</sub> Si <sub>3</sub> O <sub>9</sub>						
Nagelschmidite	Ca <sub>3</sub> ZrSi <sub>2</sub> O <sub>9</sub>					Moderate	Slow
Strontium silicate	CaTiSiO <sub>5</sub>					Poor	Very slow
Silicocarnotite	Ca <sub>5</sub> P <sub>2</sub> SiO <sub>12</sub>	65	80			Good	Moderate
Nagelschmidite	Ca <sub>7</sub> Si <sub>2</sub> P <sub>2</sub> O <sub>16</sub>					Excellent	Rapid
Strontium silicate	SrSiO <sub>3</sub>					Good	Moderate
Zinc silicate	Zn <sub>2</sub> SiO <sub>4</sub>	91	37.5			Poor	Very slow
Zinc silicate	(Sr,Ca) <sub>2</sub> ZnSi <sub>2</sub> O <sub>7</sub>						
Hydroxyapatite		80-195	75-103		0.7-1.30		
Calcium-silicate / Zirconia		395 <sup>a</sup>	81 <sup>a</sup>		4.08 <sup>a</sup>		
Dimagnesium silicate		203			2.4		
Bredigite		156	43		1.57		
Diopside		300			3.50		
Merwinite		151	31		1.72		
Monticellite		159	51		1.63		
Hardystonite		136	37		1.37		
Silicocarnotite		65	80				
Akermanite				0.53-1.13 <sup>c</sup>			
Diopside				0.2-1.36 <sup>c</sup>			
Bredigite				0.233 <sup>c</sup>			

**Notes:** The subscripts for the above are a= SPS sintering technique for ceramic; b=Porogen fabrication for porous scaffolds; c=Polyurethane foam templating for porous scaffolds; d= 3D plotting for porous scaffolds [9, 30]

## 4 Experimental design

We included results from published literature [4, 39–42] with the following inclusion criteria: 1) a variation of 45S5 Bioglass or a close variation, 2) selected carrier loaded with Vancomycin, 3) all dissolution rates determined using phosphate buffered saline (PBS), 4) PBS with pH of 7.4, and 5) test temperature of 37°C. All experiments were done in vitro. A summary of the data used and the variables documented are listed in Table 5.

The data was obtained from [4, 39–42], digitized and extrapolated with the aid of PlotDigitizer software. The digitized data was then exported in Microsoft Office, Excel for further processing. The data was used as a control to determine the release rate of a bioglass that was not coated in a polymer. The goal of the analysis was to compare the burst release of polymer coated MBG with vancomycin as well as the overall behavior of the % of the medication that was released over time in terms of an estimate of the burst release, and the rate of change of each material. The effect of different concentration of vancomycin on the burst release was based on the polymer used and total release before reaching steady state (controlled, predictable) release. The difference with the same polymer coated MBG compared to determine the overall drug release efficacy. An analysis was made with a monolayer using CS with 2mg/mL and the multilayer 8 layers applied to titanium with a total amount of 10mg/ml.

Due to the lack of identical experimental conditions used in research there were variations in the experiments as follows:

- (1) The PCL data was available for TCH (Tetrahydrocannabinol) we assumed these kinetics will describe the kinetics of vancomycin that had all of the following established guidelines;
- (2) The concentration of the medication loaded into the polymer varied on each experiment;

- (3) The coating duration range was 2.5-20 minutes;
- (4) The drying time range was 24 hours – weeks;
- (5) Thickness level ranged from 1.5-128  $\mu\text{m}$ ;
- (6) Two different fabrication methods used;
- (7) Lack of complete experimental disclosure;

These limitations establish that bioglass-coating-drug composite needs to be standardized for a given drug to optimize the release kinetics and efficacy.

## 5 Results and discussion

Although bioglass and its performance as a drug delivery carrier has been studied holistically. The interface between the bioglass-polymer-medications, and the polymer and bone are not fully understood. There also is a lack of mathematical representation of the particle, surface features determining the area, loading rate and kinetics. Simple trendline fits were applied to the trend lines to the dissolution rates to derive mathematical relationships.

As identified in the experimental design, the data from the literature with the inclusion criteria used to derive the kinetics. Table 5 summarizes the parameters used to compare and contrast the dissolution kinetics with the set of parameters. Experiments from the literature summarized in column 1 representing the studies with or without the polymer coating applied to MBG. Column 2 in this table represents numerous coating conditions applied to MBG then the vancomycin, drug, was applied. In this column we would like to identify the condition with no coating, this should serve as a control for our data. Column 3 and 4 indicate the loading rate of the drug and all experiments were conducted in vitro, respectively. Column 5 shows the MBG composition together with other columns representing similar test conditions such as dissolution solution, temperature, pH, coating and drying duration, respectively. Additional parameters summarized in the table include burst release rate, thickness and fabrication methods. Digitized data were plotted in the following Figure 3-9 together with likely zones where burst release is effective, shown by ovals, in each figure. Each of these ovals contains a specific combination of coating, polymer, and the dissolution kinetics shown. These are discussed in the order in which figures are presented.

**Table 5** Data collection carried out from the literature with various inclusion criteria used in this research

Experiment Analysis	Polymer + Vancomycin	Vancomycin (mg/ml)	In Vitro or In Vivo	Bioglass Composition (SiO <sub>2</sub> , Na <sub>2</sub> O, CaO, & P <sub>2</sub> O <sub>5</sub> )	Dissolution Solution	Temperature (°C)	pH	Coating Duration (minutes)	Drying Duration	Initial Burst Release (%)	Thickness (um)	Fabrication Method	Reference
1	PHBV	10 mg/ml	In Vitro	46.1, 24.4, 26.9, & 2.6	PBS	37°C	7.4	5 mins	24 hours	33%	1.5	FRM	[41]
1	Uncoated	10 mg/ml	In Vitro	46.1, 24.4, 26.9, & 2.7	PBS	37°C	7.4	-	-	77%	0	FRM	[41]
2	PCL-CS	25 mg/ml	In Vitro	45, 24.5, 24.5, & 6	PBS	37°C	7.4	10 min	24 hours	51%	Unknown	FRM	[42]
2	PCL-CS	50 mg/ml	In Vitro	45, 24.5, 24.5, & 7	PBS	37°C	7.4	10 min	24 hours	35%	Unknown	FRM	[42]
2	Uncoated	Unknown	In Vitro	45, 24.5, 24.5, & 8	PBS	37°C	7.4	-	-	71%	0	FRM	[42]
3	PCL	TCH at 0.5% w/v	In Vitro	45, 24.5, 24.5, & 9	PBS	37°C	7.4	2.5 min	unknown	~38%	min. of 2-5	FRM	[4]
4	CS	2 mg/ml Vanc	In Vitro	45, 24.5, 24.5, & 10	PBS	37°C	7.4	10 min	Unknown	20%	~ 55	EPD	[39]
4	CS-BG	2 mg/ml Vanc	In Vitro	45, 24.5, 24.5, & 11	PBS	37°C	7.4	10 min	Unknown	40%	~ 55	EPD	[39]
5	CS-BG Monolayer	2 mg/ml Vanc	In Vitro	45, 24.5, 24.5, & 12	PBS	37°C	7.4	10 min	up to 2 weeks	40%	Unknown	EPD	[40]
5	CS-BG (Multilayer)	0.5-2 mg/mL	In Vitro	45, 24.5, 24.5, & 13	PBS	37°C	7.4	20 min	up to 2 weeks	8%	~128	EPD	[40]

Notes: PHBV: Poly(3-hydroxybutyrate-co-3-hydroxyvalerate); CS: Chitosan; PCL: polycaprolactone; BG: Bioactive Glass; TCH: Tetrahydrocannabinol; PBS: Phosphate-buffered saline; FRM: Foam Replication Method; EPD: Electrophoretic Deposition.

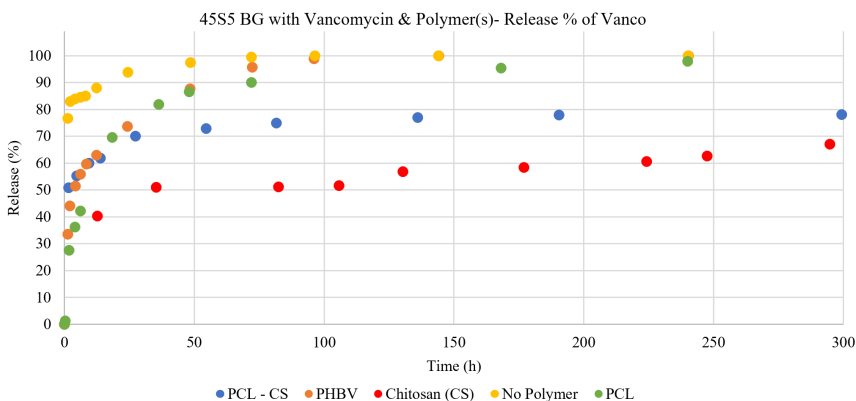


**Figure 3** Release percentages of PCL-CS, PHBV, Chitosan, no polymer, and PCL (data from Table 5)

Figure 3 shows that uncoated MBG has a faster release rate compared to when MBG was coated with polymer, demonstrating that this is the least desirable material. There is a sudden burst release, in the 20% of the time leading all the way to 100% dissolution. Chitosan appears



to have a slower release rate compared to the other polymers, which is more desirable. Possible causes for the superior release rate may be attributed to the wt. loss of the material with increased drying time. The PCL used TCH whereas the other used Vancomycin. PCL had the least amount of coating as shown in Table 5.

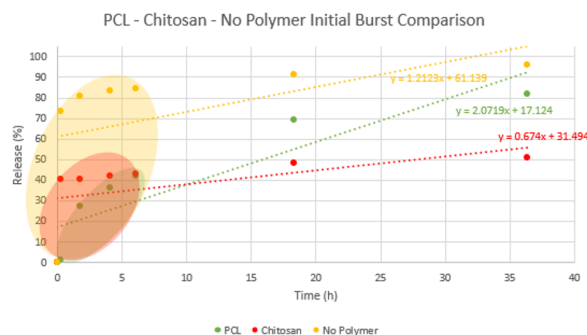


**Figure 4** Initial Bust Release: PCL vs. chitosan vs no polymer, data from Table 5.

The rate of change for the PCL is approximately greater by 0.5 % per hour compared to the no polymer and chitosan, PCL-CS. This can be contributed to the differences in the rate of change for the PCL release rate. This is not seen in the initial release rate. At approximately 10 hours an intersection of the release rate occurs for the chitosan and the PCL. After 10 hours the positive steep slope is observed for the PCL. The no polymer and the chitosan appear to have behavior in which the slope is parallel to one another. An overlap oval between the chitosan and PCL is noted between 0 – approximately 5 hours and from 0% to approximately 50% release rate. Schematically an ovals is an estimate of the initial burst release based on the numerical data generated with the use of PlotDigitizer. The top edge of the oval was determined based on the point where the release % begins to stop and starts to reach steady state to provide a more predictable rate of the medication release. It is likely that based on the rate of change the first data point can affect the rate of change of the vancomycin because the more that is released in the initial burst release results in less medication being available over time to be released.

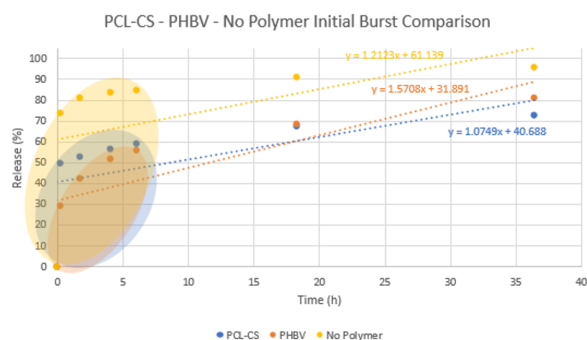


**Figure 5** Initial Bust Release: PCL-CS vs. PHBV vs no polymer, data from Table 5.

PHBV and PCL-CS have much lower initial release values compared to the no polymer. The ovals show that by the time that the estimated burst release is complete, the PCL-CS and PHBV nearly cross at ~60% of time. This contributes to why the release rate in the beginning stages of the experiment are larger in the PHBV coated bioactive glass compared to the PCL-CS. Although the PCL-CS initial release value was greater, the lower rate allowed the PHBV coating to pass the overall release of the drug. The composition is slightly different which could impact the initial value but as seen from in Figure 4 and 5, respectively, the rate stays quite similar.

Under the same conditions, the initial burst release of the 25 mg/ml Vancomycin is ~15% higher than the 50 mg/ml of Vancomycin. The overall release of the drug was ~20% higher for the 25 mg/ml. This shows that the lower the amount of drug, the higher percentage of the drug is being used. This could be due to oversaturation of Vancomycin but if we were to take the percentages and multiply them to each drug composition, it shows that the amount of drug in mg/ml is still higher than the amount if the drug amount was higher. The rate remains quite similar between the amounts which means that the higher amount of drug slows the total amount of drug that is released in each experiment. This could be due to the mechanical factors and the oversaturation factors. Additional factors that may be considered include mechanical properties increase with the higher drug loading rate, causing it to dissolve slowly as the diffusion and other parameters dictate the dissolution.

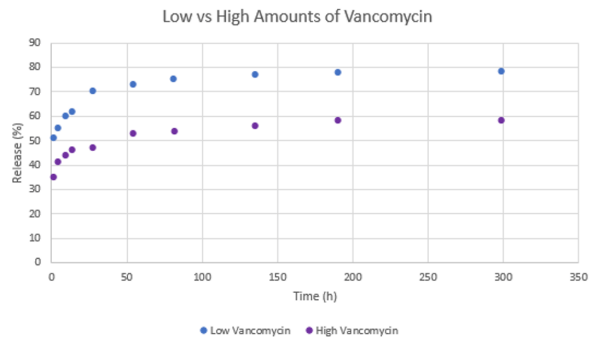


**Figure 6** The overall drug release comparison of PCL-CS polymer at 25 mg/ml and 50 mg/ml of Vancomycin data from Table 5.

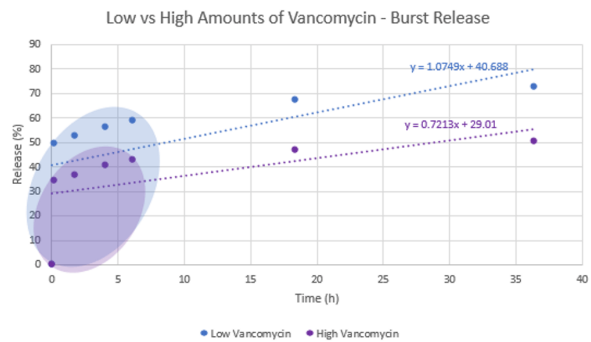


**Figure 7** The initial burst release for the PCL-CS polymer at 25 mg/ml and 50 mg/ml of Vancomycin, data from Table 5.

The initial burst release of the 25 mg/ml of Vancomycin is much lower and has a smaller rate. This shows that the initial burst value becomes lower when higher amounts of vancomycin present. This is similar findings to Figure 5 data but specifically covering the burst release. The rate is also quite similar pointing to the same findings as Figure 5.

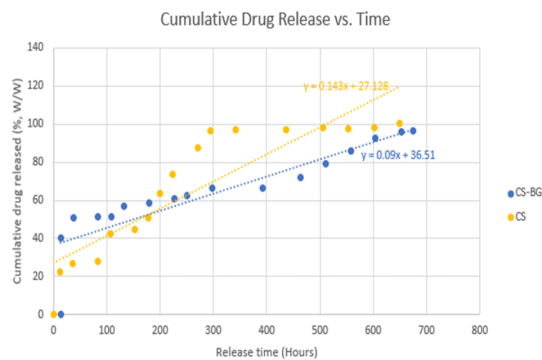


**Figure 8** Comparison of Chitosan coating of 45S5 BG with Vancomycin, data from Table 5.

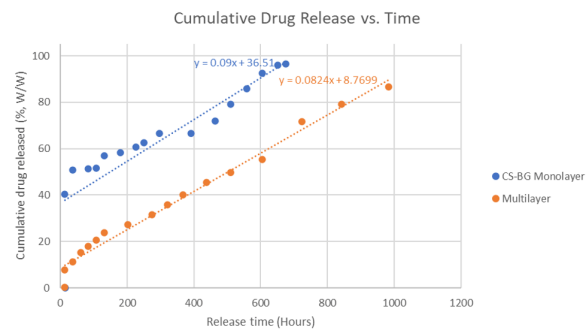


**Figure 9** The effects of multiple layers and compositions to single layer chitosan 45S5 BG data from Table 5.

The initial burst release value of the chitosan without the 45S5 BG present is half of the value when the 45S5 BG is present. Also, without the bioactive glass present, the overall rate of release was nearly double the chitosan with 45S5 BG which means that without the BG it had reached nearly half as fast as with the BG. Therefore, the impact of the 45S5 bioactive glass increases the initial release burst of increasing dissolution. At around 200 hours the release percentage of the bioglass included drug release is passed by the drug release without bioglass because the rate is far greater. At around 300 hours, the chitosan without bioactive glass reaches near full distribution of the drug while the test with the bioactive glass present doesn't reach that until ~650 hours. In conclusion the bioactive glass allows for a greater initial release of a drug but slows the release rate to allow drug distribution for longer periods of time.

For the multilayer the layers are as follows: 1) CS-0.5 mg/ml VAN, 2) CS-BG-0.5 mg/ml VAN, 3) CS-1 mg/ml VAN, 4) CS-BG-1 mg/ml VAN, 5) CS-1.5 mg/ml VAN, 6) CS-BG-1.5 mg/ml VAN, 7) CS-2 mg/ml VAN, 8) CS-BG-2 mg/ml VAN. The data shows that the initial release value is nearly 30% higher for the single layer. The multilayer compared to any initial value from Figure 3-8 and Table 5 show that this is by far the lowest initial release value. Also, the rate of release of each experiment was quite similar and that the multilayer took about 250 hours longer to approach complete drug release. This means that the distribution of the drug will be prolonged with many layers being applied. Since the rate is similar the multilayer only played a role in the initial release value which alters the overall release as time passes.

## 6 Conclusions

Bioactive glass has shown superior capabilities in drug delivery compared to traditional carriers. The data compiled in this paper shows that polymer coated 45S5 Bioglass® loaded with vancomycin achieves controlled time release for more than 50%. Since MBG continues to be a preferred carrier with numerous combinations; pore volume, size, coating, doped with ions, medications, and other physical conditions, the effectiveness of the present carrier is a function of many parameters. For a given loading efficiency of 5-15% the burst release % for day 1 remained 15-30% for given surface area, pore volume and pore size of 3.5 to 5 nm. The mechanical properties summarized in this paper are compared with the drug release kinetics. In general, for a given fracture toughness and compressive strength, the ratio of Young's modulus to bending strength around 250 determined poor apatite mineralization resulting in slow release. As this ratio increased the apatite mineralization and dissolution rate increased. Doping MBG with ions enhanced the drug efficacy to treat a particular condition, for example, silver. Polymer coated MBG exhibited slower dissolution rate than uncoated MBG. Dissolution time increased with the drug loading rate, drying time of the coating, multi-layer coats of drug and polymer for the drug studied in this paper to more than 50%.

## References

- [1] Bairo F, Hamzehlou S and Kargozar S. Bioactive Glasses: Where Are We and Where Are We Going?. *Journal of Functional Biomaterials*, 2018, **9**(25): 1-27. <https://doi.org/10.3390/jfb9010025>
- [2] Jones RJ, Brauer DS, HupaL, *et al.* Bioglass and Bioactive Glasses and Their Impact on. *International Journal of Applied Glass Scienc*, 2016, **7**(4): 423-434. <https://doi.org/10.1111/jjag.12252>
- [3] Bairo F, Fiume E, Barberi J, *et al.* Processing methods for making porous bioactive glass-based scaffolds-A state-of-the-art review. *American Ceramic Society*, 2019, **16**: 1762-1796. <https://doi.org/10.1111/jjac.13195>
- [4] Brauer ds. Bioactive Glasses-Structure and Properties. *Bkioactive Glasses*, 2015, **54**: 2-24. <https://doi.org/10.1002/anie.201405310>
- [5] Kaur G, Kumar V, Bairo F, *et al.* Mechanical properties of bioactive glasses, ceramics, glass-ceramics and composites: State-of-the-art review and future challenges. *Materials Science and Engineering: C*, **104**(C): 109895-109895. <https://doi.org/10.1016/j.msec.2019.109895>
- [6] Izquierdo-Barba I and Vallet-Regí M. Mesoporous bioactive glasses: Relevance of their. *Biomedical Glasses*, 2015, **1**(1): 140-150. <https://doi.org/10.1515/bglass-2015-0014>
- [7] Migneco C, Fiume E, E Verné, *et al.* A Guided Walk through the World of Mesoporous Bioactive Glasses (MBGs): Fundamentals, Processing and Applications. *Nanomaterials*, 2020, **10**(12): 2571. <https://doi.org/10.3390/nano10122571>
- [8] Xia W and Chang J. Bioactive glass scaffold with similar structure and mechanical properties of cancellous bone. *Journal of Biomedical Materials Research Part B Applied Biomaterials*, 2010, **95B**(2): 449-455. <https://doi.org/10.1002/jbm.b.31736>

- [9] Cabanas-Polo S and Boccaccini AR. Understanding Bioactive Glass Powder Suspensions for Electrophoretic Deposition of Bioactive Glass-Polymer Coatings. *Journal of The Electrochemical Society*, 2015, **162**(11): 3077-3083.  
<https://doi.org/10.1149/2.0211511jes>
- [10] Wu C and Chang J. Mesoporous bioactive glasses: structure characteristics, drug/growth factor delivery and bone regeneration application. *Interface Focus*, 2012, **2**(3): 292-306.  
<https://doi.org/10.1098/rsfs.2011.0121>
- [11] Li Y, Liu YZ, Long T, *et al.* Mesoporous bioactive glass as a drug delivery system: fabrication, bactericidal properties and biocompatibility. *Journal of Materials Science: Materials in Medicine*, 2013, **24**(8): 1951-1961.  
<https://doi.org/10.1007/s10856-013-4960-z>
- [12] Subhapradha N, Abudhahir M, Aathira A, *et al.* Polymer coated mesoporous ceramic for drug delivery in bone tissue engineering. *International Journal of Biological Macromolecules*, 2018, **110**: 65-73.  
<https://doi.org/10.1016/j.ijbiomac.2017.11.146>
- [13] Sigma M. Drug Delivery FAQs.  
<https://www.sigmaldrich.com>
- [14] Xiao H and Brazel CS. On the importance and mechanisms of burst release in matrix-controlled drug delivery systems. 2001, **73**(2-3): 121-136.  
[https://doi.org/10.1016/S0168-3659\(01\)00248-6](https://doi.org/10.1016/S0168-3659(01)00248-6)
- [15] Quantachrome Instruments. Measuring Particle Surface Area by Gas Sorption.  
<https://www.quantachrome.com>
- [16] Dictionary.com. Definition of volume. Available: <https://www.dictionary.com>
- [17] María C, Tess G, Katilayne V, *et al.* Photopolymerization for Filling Porous Ceramic Matrix: Improvement of Mechanical Properties and Drug Delivering Behavior. *Polymer Composites*, 2018, **40**(4): 1654-1662.  
<https://doi.org/10.1002/pc.24914>
- [18] Hench LL. The story of Bioglass. *Journal of Materials Science Materials in Medicine*, 2006, **17**(11): 967.  
<https://doi.org/10.1007/s10856-006-0432-z>
- [19] Wei Li, Ding Y, Rai R, *et al.* Preparation and characterization of PHBV microsphere/45S5 bioactive glass composite scaffolds with vancomycin releasing function. *Materials Science and Engineering: C*, 2014, **41**: 320-328.  
<https://doi.org/10.1016/j.msec.2014.04.052>
- [20] Motealleh A, Eqtesadi S, Perera FH, *et al.* Understanding the role of dip-coating process parameters in the mechanical performance of polymer-coated bioglass robocast scaffolds. *Journal of the Mechanical Behavior of Biomedical Materials*, 2016, **64**: 253-261.  
<https://doi.org/10.1016/j.jmbbm.2016.08.004>
- [21] Nawawi N, Alqap ASF and Sopyan L. Recent Progress on Hydroxyapatite-Based Dense Biomaterials for Load Bearing Bone Substitutes. *Recent Patents on Materials Science*, 2011, **4**(1): 63-80.  
<https://doi.org/10.2174/1874465611104010063>
- [22] Combes C, Cazalbou S and Rey C. Apatite Biominerals. *Minerals*, 2016, **6**(2): 2-25.  
<https://doi.org/10.3390/min6020034>
- [23] Kaur G. *Biomedical, Therapeutic and Clinical Applications of Bioactive Glasses*, Duxford: Woodhead Publishing, 2019.
- [24] Zhang X, Zeng D, Li N, *et al.* Functionalized mesoporous bioactive glass scaffolds for enhanced bone tissue regeneration. *Scientific Reports*, 2016, **6**: 19361.  
<https://doi.org/10.1038/srep19361>
- [25] University of Cambridge. Mechanical properties of bone.  
<https://www.doitpoms.ac.uk>
- [26] Su J, Cao L, Yu B, *et al.* Composite scaffolds of mesoporous bioactive. *International Journal of Nanomedicine*, 2012, **7**: 2547-2555.  
<https://doi.org/10.2147/IJN.S29819>
- [27] Ramiro-Gutiérrez ML, Will J and Boccaccini AR. Reticulated bioactive scaffolds with improved textural properties for bone tissue engineering: Nanostructured surfaces and porosity. *Journal of Biomedical Materials Research*, 2014, **102**(9): 2982-2992.  
<https://doi.org/10.1002/jbm.a.34968>
- [28] Cauda V, Fiorilli S, Onida B, *et al.* SBA-15 ordered mesoporous silica inside a bioactive glass-ceramic scaffold for local drug delivery. *Journal of Materials Science Materials in Medicine*, 2008, **19**(10): 3303-3310.  
<https://doi.org/10.1007/s10856-008-3468-4>
- [29] Boffito M, Pontremoli C, Fiorilli S, *et al.* Injectable Thermosensitive Formulation Based on Polyurethane Hydrogel/Mesoporous Glasses for Sustained Co-Delivery of Functional Ions and Drugs. *Pharmaceutics*, 2019, **11**(10): 1-20.  
<https://doi.org/10.3390/pharmaceutics11100501>
- [30] Yao Q, Noeaid P, Roether JA, *et al.* Bioglass-based scaffolds incorporating polycaprolactone and chitosan coatings for controlled vancomycin delivery. *Ceramics International*, 2013, **39**(7): 7517-7522.  
<https://doi.org/10.1016/j.ceramint.2013.03.002>

- [31] Rivadeneira J and Gorustovich A. Bioactive glasses as delivery systems for antimicrobial agents. *Journal of Applied Microbiology*, 2016, **122**(6): 1424-1437.  
<https://doi.org/10.1111/jam.13393>
- [32] Huirache-Acua R, Nava R, Peza-Ledesma CL, *et al.* SBA-15 Mesoporous Silica as Catalytic Support for Hydrodesulfurization Catalysts—Review. *Materials*, 2013, **6**(9): 4139-4167.  
<https://doi.org/10.3390/ma6094139>
- [33] Agrawal CM, Ong JG, Appleford MR, *et al.* Introduction to Biomaterials: Basic Theory with Engineering Applications, United Kingdom: Cambridge University Press, 2014.  
<https://doi.org/10.1017/CBO9781139035545>
- [34] Britannica. Young's modulus. Encyclopedia Britannica.  
<https://www.britannica.com>
- [35] Britannica. compressive strength test. Encyclopaedia of Britannica.  
<https://www.britannica.com>
- [36] Pawelec KM, White AA and Best SM. Properties and characterization of bone repair materials. in *Bone Repair Biomaterial 2nd edition*, Kidlington, Woodhead Publishing Series in Biomaterials, 2019, 65-102.  
<https://doi.org/10.1016/B978-0-08-102451-5.00004-4>
- [37] O'Hara R and Dunne BN. 2-Injectable calcium phosphate cements for spinal bone repair. in *Biomaterials for Bone Regeneration: Novel Techniques and Applications*, Kidlington, Woodhead Publishing, 2014, 26-61.  
<https://doi.org/10.1533/9780857098104.1.26>
- [38] Johnson L. How to Calculate Flexural Strength.  
<https://sciencing.com>
- [39] Ordikhani F and Simchi A. Long-term antibiotic delivery by chitosan-based composite coatings with bone regenerative potential. *Applied Surface Science*, 2014, **317**: 56-66.  
<https://doi.org/10.1016/j.apsusc.2014.07.197>
- [40] Ordikhani F, Zustiak SP and Simchi A. Surface Modifications of Titanium Implants by Multilayer Bioactive Coatings with Drug Delivery Potential: Antimicrobial, Biological, and Drug Release Studies. *Journal of Medicine*, 2016, **68**: 1100-1108.  
<https://doi.org/10.1007/s11837-016-1840-2>
- [41] Wei LA, Pn A, Jar B, *et al.* Preparation and characterization of vancomycin releasing PHBV coated 45S5 Bioglass-based glass–ceramic scaffolds for bone tissue engineering - ScienceDirect. *Journal of the European Ceramic Society*, 2014, **34**(2): 505-514.  
<https://doi.org/10.1016/j.jeurceramsoc.2013.08.032>
- [42] Yao Q, Noeaid P, Roether JA, *et al.* Bioglass-based scaffolds incorporating polycaprolactone and chitosan coatings for controlled vancomycin delivery. *Ceramics International*, 2013, **39**(7): 7517-7522.  
<https://doi.org/10.1016/j.ceramint.2013.03.002>